Chapter 13
Solitons and Charge Transport in Triangular and Quadratic Crystal Lattices

A.P. Chetverikov, W. Ebeling and M.G. Velarde

Abstract We study solitons and solectrons and their time and space evolution in triangular and quadratic anharmonic lattices with Morse interactions. First we offer computational evidence of the possibility of long lasting, supersonic lattice solitons moving along crystallographic axes. On the basis of the dispersion equations we postulate appropriate evolution equations of Boussinesq and Kadomtsev-Petviashvili (KP) type. Adding electrons to the lattice we find solectron bound states in computer simulations corresponding continuous KP and nonlinear Schrödinger equations. As a follow-up of the above, we also offer computational evidence of the possibility of supersonic, almost losses-free transfer or transport of electrons along crystallographic axes. Finally we show how electrons can be controlled and transported by such acoustic solitonic waves and how electron-surfing occurs at the nanoscale.

13.1 Introduction

Applications of nonlinear dynamics appear, more and more, in a variety of fields of science and, in particular, in several branches of Physics from hydrodynamics to optics, Bose-Einstein condensates, etc. [2]. The possibility of controlling and transporting, e.g., charges or holes at relatively very high velocities (km/s, Å/ps) and over long distances (from, say, nm to mm) has recently being explored both in theory, with computer simulations, and in experiments. The latter have shown how electrons

A.P. Chetverikov (✉)
Department of Physics, Saratov State University,
Astrakhanskaya 83, 410012 Saratov, Russia
e-mail: chetverikovap@info.sgu.ru

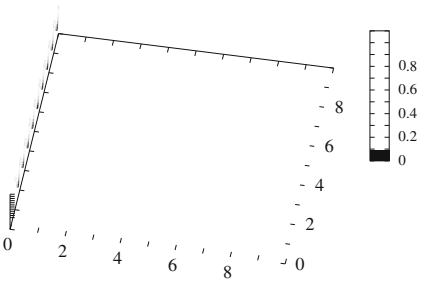
W. Ebeling

can *surf* on appropriate acoustic waves, excited in adequate substrates. Such electron surfing occurs at the nano- and at the macro-level [7, 9, 12, 17, 23, 32, 35, 42, 52, 56]. At the macro-level suffices to use a piezoelectric material like a GaAs layer, where a strong enough acoustic, linear or much better soliton, wave generates the appropriate corresponding polarization field wave able to carry the charge. At the nano-level a strong enough mechanical or electrical local perturbation, e.g., generated at the tip contact of an AFM, can excite acoustic solitons in anharmonic lattice crystals like PDA and other related crystals. Let us also mention the observation of localized excitations (discrete breathers, quodons) in layered structures like muscovite mica [30, 31, 43] and *stripes* in cuprate layers [20, 26, 27, 34, 41, 45, 49, 50, 54]. Of particular interest are collective phenomena in two-dimensional (2d) lattices, which are so far little explored. In the present work we study soliton-like collective excitations in 2d systems. Significant works on the theory are due to Kadomtsev, Petviashvili, Zakharov and others [1, 10, 11, 14, 15, 24, 25, 28, 29, 33, 36, 37, 40, 44, 55].

In our simulations we consider systems of a few hundred atoms on a plane interacting with one or a few added, excess electrons. Earlier we have discussed various consequences of the interaction between electrons and strongly localized lattice excitations of soliton-type in one-dimensional (1d) and 2d lattices [7, 9, 12]. For the electron dynamics we used the tight-binding approximation (TBA) and for the lattice particles a classical Hamiltonian with Morse interactions. As a result of this mixed classical-quantum dynamics we could show that the electrons "like" to follow the trajectories of the soliton-like lattice excitations. In the 1d case we have predicted several interesting phenomena, in particular the "vacuum-cleaner" effect, i.e., the electron probability density is gathered by solitons which along their trajectory act as long range attractors [16, 22, 51]. Noteworthy is that these excitations move in general with *supersonic* velocity or velocities a bit below the sound velocity depending on parameter values, on the initial conditions and on the electron-lattice interaction. This means that electrons bound to lattice solitons (in short called *solectrons*) can move with supersonic or slightly subsonic velocities of the order of km/s (Å/ps).

13.2 Excitations in Square Lattices

Square lattices in 2d are closely related to 1d lattices since they may be considered as just two perpendicular crossed 1d-lattices (Fig. 13.1, left panel). Each atom has four nearest neighbors and we have two crystallographic axes. We expect therefore two quasi 1d excitations along the crystallographic axes. Depending on the forces, there might be problems with he stability of square lattices, and this we will discuss in the next section. Assuming the atoms have the coordinates $\mathbf{r_i}$ and the velocities $\mathbf{v_i}$ the Hamiltonian of our 2d system is


0.8
0.6
0.4
0.2
0
8
6
4
2
0
0
2
4
6
8

particle under the influence of all possible forces. Our simulation algorithm corresponds to a molecular dynamics code, i.e. the particles are not fixed to any lattice node but may move freely through the system, exchanging places with neighbors etc. Rather than using Cartesian coordinates x and y, we use dimensionless complex coordinates $Z = (x + iy)/\sigma$. Then the initial classical Newton deterministic equations corresponding to the lattice Hamiltonian (13.1) including also friction and random forces yield to a Langevin dynamics for the lattice units

$$\frac{d^2 Z_i}{dt^2} = \sum_k F_{ik}(|Z_{ik}|) z_{ik} + \left[-\gamma \frac{dZ_i}{dt} + \sqrt{2D_v} \left(\xi_{ix} + i\xi_{iy} \right) \right], \qquad (13.3)$$

where the index i identifies a particle among all N particles of the ensemble, γ is a friction coefficient, D_v defines the intensity of stochastic forces, $\xi_{ix,y}$ denote statistically independent generators of the Gaussian noise. $T = mD_v/\gamma$ (Einstein's relation). $Z_{ik} = Z_i - Z_k$ and $z_{ik} = (Z_i - Z_k)/|Z_i - Z_k|$ is the unit vector defining the direction of the interaction force F_{ik}, corresponding to the Toda or Morse potential, between the ith and the kth atoms in the lattice. Let us first study analytical representations for the noise-free case. In the case of Toda interactions exists a special exact analytical solution for the square lattice by using the functions found by Toda analytically solving the 1d-equations [1, 28, 40, 44]. The Toda solutions remain valid for the special case that the initial conditions and the corresponding excitations are strictly parallel to one axis, say the x-axis. Let n, m be the numbers denoting the nodes in x- and y-direction and let us define the lattice compressions in x-direction by

$$\rho_{n,m}(t) = x_n(t) - x_{n+1}(t) - \sigma. \qquad (13.4)$$

Note that there are no compressions in y-direction due to the assumed parallel dynamics inside the rows. Then with appropriate initial conditions an exact solution is given by the Toda profile running along the x-axis

$$\rho_{n,m}(t) = \frac{1}{b_T} \ln \left[1 + \frac{\sinh^2(\kappa)}{\cosh^2(\kappa n - \beta t)} \right]; \qquad \beta = \sinh(\kappa). \qquad (13.5)$$

For small amplitudes this gives

$$\rho_{n,m}(t) \simeq \frac{1}{b_T} \frac{\sinh^2(\kappa)}{\cosh^2(\kappa n - \beta t)}. \qquad (13.6)$$

As earlier noted, for Morse systems we find empirically a good description of the observed profile for $b \simeq b_T/3$. The constant κ is defined by the energy of the soliton. In the continuum limit this gives the well known soliton profile [17, 44, 56]

$$\rho(x, y, t) = \rho_0 \mathrm{sech}^2(\kappa\xi), \qquad \xi = (x \pm v_s t)/\sigma, \tag{13.7}$$

where v_s is the soliton velocity. The soliton represented by (13.7) is a special solution, representing a "line-soliton", of the so-called KP-equation. The Kadomtsev-Petviashvili equation is an extension of the 1d Boussinesq-Korteweg-de Vries (BKdV) equation and reads in a standard form [1, 24, 25, 28, 33]:

$$\frac{\partial}{\partial x}\left[\frac{\partial}{\partial t} + \frac{\partial^3}{\partial x^3}\right]\rho(x, y, t) = \frac{\partial^2}{\partial y^2}\rho(x, y, t) + 3\frac{\partial^2}{\partial x^2}\rho^2(x, y, t). \tag{13.8}$$

Line solitons are extended rectilinear wave fronts localized perpendicular to the propagation direction, as also shown by the computer simulations [10, 11].

Let us discuss the method of computer simulations in more detail. We solve numerically the equations of motion for the complex coordinates $Z_i(t)$ taking into account only those atomic units satisfying the condition $|Z_i - Z_k| < 1.5$. The dynamics of the atoms is considered to take place inside a rectangular cell $L_x \cdot L_y$ with periodic boundary conditions and depending on the symmetry of an initial distribution of units and their number $N \simeq 400$. As initial condition we assume a lattice compression and velocity profiles corresponding to the analytical form of a 1d Toda soliton [1, 28, 40, 44] in a given lattice row. The other lattice units remain at their equilibrium positions on the given lattice [10, 11]. As shown by Remoissenet [40], a broad spectrum of initial excitations, as e.g. excitations of rectangular profiles are able to create solitons or cnoidal waves. For this reason we have experimented with a broad range of initial conditions. For example we gave initially a suitable high momentum to one lattice atom in the direction of one of the crystallographic axes in such a way that a successful start of a soliton was observed. This way we found that not only Toda profiles but also simpler initial conditions as pushing initially just one lattice particle may be sufficient to create a soliton due to the suitable stiffness of the exponential repulsion.

For visualization and tracking the atomic densities we modeled the atoms as little spheres with "cores" represented by Gaussian distributions centered at each lattice site:

$$\rho(Z, t) = C \sum_{|Z - Z_i(t)| < 1.5} \exp\left[-\frac{|Z - Z_i(t)|^2}{2\lambda^2}\right], \tag{13.9}$$

where C is an *ad hoc* scaling factor thus permitting depicting $\rho(Z, t)$ in units of C. Using data about trajectories of particles $Z_n(t)$ and their velocities we can calculate the lattice atom distribution $\rho(Z, t)$. The value of the parameter λ is chosen in such a way that the heights of each Gaussian peak corresponding to all lattice atoms take the value unity. The local excess above unity indicates a corresponding local lattice "compression" or overlapping of Gaussians, when the lattice is perturbed. To make the picture much clear we introduce an "extra density" $\rho_{ex} = \rho - \rho_c$

with $\rho_c = 1 - \delta(\delta \ll 1)$. Varying δ allows observation of regions with different compression levels/Gaussian overlappings. Furthermore, to clearly distinguish moving "local compressions" we use $\rho_{ac} = \sum_k \rho_{ex}(kt_{ac})$, where t_{ac} is the time interval for producing $\rho_{ex}(x, y, kt_{ac})$, with $k = 1, 2, \ldots, K$, $K = t_{sim}/t_{ac}$. The parameter t_{sim} is our running computer simulation time interval. Accordingly, following the space-time evolution of $\rho_{ac}(x, y, t)$ solitons appear as tracks of moving lattice particles/atoms as a kind of bubble chamber traces. The "localized compressions" appear as bright areas of increasing brightness if the localized compression is pinned. In Fig. 13.2 we show a track of the running excitation (in such "bubble chamber representation", left panel) which was created by pushing just one atom in the direction of the crystallographic axis x. We show the space and time evolution of the initial soliton density peak for the time interval $\Delta t = 4$ (measured in units of $1/\omega_0$, as earlier said). The parameter values of the potential are $b\sigma = 7$, $\lambda = 0.3$. The Langevin source corresponds to a rather low temperature, $T = 0.001$ (in dimensionless units). This corresponds to the mean kinetic energy of a particle $< T_{kin} >$ reaching the value T. The soliton is moving along a crystallographic axis and was excited by a strong pulse of velocity $1.5v_0$ imposed at $t = 0$ to the 4th atom $n = 4$ in the 10th row with rather high energy $1.125\, mv_0^2(b\sigma)^2$. Here v_0 is the sound velocity in a corresponding 1d-lattice. The high-energetic soliton excited this way is quite long lasting in its motion along the chosen crystallographic axis. Transverse excitations and thermal collisions due to the source term in the Langevin equation do not play a significant role in the interval of observation (4 time units ω_0^{-1}). The phenomena studied in our simulations remind very much the discrete moving breathers observed by Marin et al. [30, 31, 43] for a wide range of nonlinear 2d lattices. These authors have shown that breather excitations propagate along lattice directions at subsonic speeds and are rather robust. The results suggested broader applications including the track formation in some mica minerals and stripes in cuprates [20, 26, 27, 30, 31, 34, 41, 43, 45, 54]. From the length of the cumulative path and the time interval we may estimate the velocity of the excitations shown in Fig. 13.2. It appears that this strong local compression moves with velocity about $3v_{sound}$ with a lifetime of at least several time units ω_0^{-1}. In the 2d triangular Morse lattice v_{sound} is slightly above 1 in our units, which here is the 1d sound velocity. Solitonic excitations move a few picoseconds with nearly unaltered profile and just this robustness is the reason that we can identify them with the proposed visualization method. Losses due to scattering and radiation of linear waves are quite low, due to the nearly integrable character of the problem. Note that the 2d solitons observed here, are not line solitons but localized solitons similar to the so-called lump solutions of the KP equations [29, 33]. Looking at the transverse direction we find that the oscillations of the atoms in the rows adjacent to the row of maximal activity of the soliton oscillate in antiphase reminiscent of 1d discrete breathers (Fig. 13.3) [3, 13, 21, 30, 31, 43]. We will show in the next section that the similarity to KP-solitons is so striking that we decide to qualify them as 2d-solitons [10, 11].

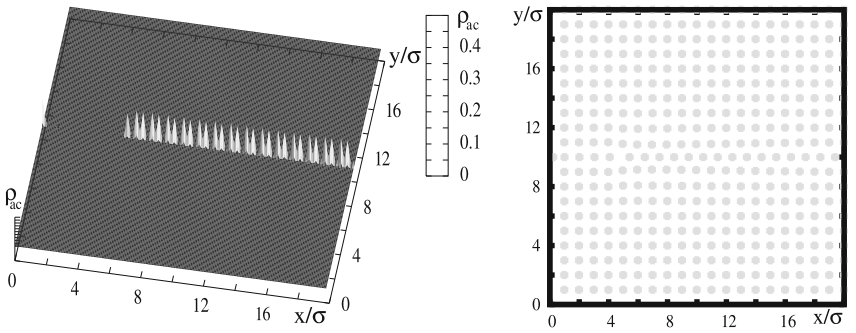


Fig. 13.2 *Square lattice* The core density of the lattice atoms, left panel, and positions of point particles at the latest time instant of simulation $t = 4$, right panel, are shown in the course of time. A lattice soliton is excited by a strong pulse in $x-$ direction with velocity $1.5v_0$ imposed to one lattice particle located not far from the left border along to the 4th atom in the row 10. A track of the excitation (in "bubble chamber representation") of the running soliton density is represented for the time interval $\Delta t = 4$ (measured in units of $1/\omega_0$) in "bubble chamber sequence" as time proceeds. *Parameter values* $N = 400$, $b\sigma = 7$, $\lambda = 0.3$, and $T = 0.001$ (in units of $2D$)

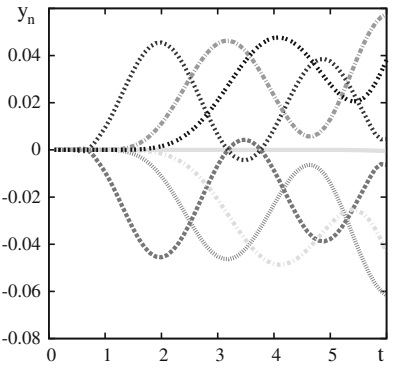


Fig. 13.3 *Square lattice* Time evolution in the atomic rows adjacent to the (*central*) one in which a high energy soliton-like excitation is running (*red* soliton row; *dark blue and green* nearest row; *light blue and pink*: next-nearest row, etc). The period of oscillations is below $3\omega_0$

A specific property of our solitonic excitations in square lattices is that potential energy may be released during propagation. Therefore the solitonic propagation may leave irreversible traces (see Fig. 13.2). The trajectories may be self-sustained and sometimes might be extremely long. As mentioned already, similar trajectories were observed for example as long black stripes in natural crystals of muscovite mica [13]. In theoretical work of Marin et al. [30, 31, 43] such stripes were interpreted as moving breathers. Our numerical experiments suggest that the tracks in muscovite mica could be interpreted also as high-energetic solitons which are very robust when running along crystallographic axes.

13.3 Dispersion Relation for Two-Dimensional Excitations and KP Equation

For a linear 1d-lattice the dispersion equation for excitations in x-direction reads

$$\omega^2 = 4\sin^2\left(\frac{1}{2}k\right). \tag{13.10}$$

Recall that here the frequency of the linear oscillations ω_0 is the unit of frequency and the reciprocal lattice length $1/\sigma$ is the wave number unit.

Let us search now for appropriate wave equations. Denoting the continuum limit of the strain $z_n = x_n - x_{n-1} - \sigma$ as the compression density $\rho(x,t)$ we arrive at a partial d.e. which was obtained already in 1877 by Boussinesq for the description of hydrodynamic waves (we purposedly take the equation for waves travelling in both directions) [1, 28]:

$$\left[\frac{\partial^2}{\partial t^2} - v_0^2\left(\frac{\partial^2}{\partial x^2} + \frac{1}{12}\frac{\partial^4}{\partial x^4}\right)\right]\rho(x,t) = \frac{\gamma}{\kappa}\frac{\partial^2}{\partial x^2}\rho^2(x,t), \tag{13.11}$$

with the dispersion relation

$$\omega^2 = k^2 v_0^2\left[1 - (k^2\sigma^2)/12 + \ldots\right]. \tag{13.12}$$

In the lowest approximation the Boussinesq equation reduces to the standard linear wave equation, which is solved by two plane waves $\rho(\xi)$ depending on the dimensionless running coordinate $\xi = (x \pm v_0 t)/\sigma$ where, as said before, v_0 is the sound velocity. For the nonlinear Boussinesq equation there are two solutions for the continuous density

$$\rho(x,t) = \rho_0 \mathrm{sech}^2(\kappa\xi), \qquad \xi = (x \pm v_s t)/\sigma, \tag{13.13}$$

in agreement with the approximation (13.7) written above. The 1d solitons described by (13.13) correspond to long wave length and hence to small wave vectors k. In the 2d-case we expect in agreement with the previous section, waves which have a similar profile in x-direction but are extended also in y-direction. Indeed there are excitations in 2d which are either line solitons or lump solitons. Both are in x-direction like the BKdV solitons. Line solitons are extended in y-direction and lump solitons have in y-direction an envelope which is like a Gaussian.

We will show now that the KP-equation describes both phenomena. Let us consider again the case of the simplest 2d quadratic lattice. A straightforward additive combination of two linear lattices would correspond to the dispersion relation

$$\omega^2 = 4\sin^2\left(\frac{1}{2}k_x\right) + 4\sin^2\left(\frac{1}{2}k_y\right). \tag{13.14}$$

The problem with the KP-solutions, which describe observed 2d-phenomena, is that they are not symmetric along x and y. Hence (13.14) needs some further treatment. The soliton-like waves we have found in our computer simulations run along the x-axis like a soliton but, as earlier noted, in the direction of the y-axis the neighboring lattice units oscillate in anti-phase like discrete breathers with amplitudes slowly decreasing along y. Because in the transverse direction the 2d-solitons behave like discrete breathers, we should use for the dispersion relation a "soliton-like" expansion along the axis x and a "breather-like" expansion into a series along the axis y. We assume that in $k_x - k_y-$ space the essential parts of the 2d-soliton dynamics appear in the region

$$|k_x| \ll 1, \qquad k_y = \pi + \Delta k_y, \qquad |\Delta k_y| \ll 1, \qquad \omega \simeq 2. \tag{13.15}$$

The significant region is the left upper corner in the first Brillouin zone. Accordingly we may use the expansion

$$\omega^2 = 4\left[\frac{1}{4}k_x^2 - \frac{1}{48}k_x^4\right] + 4\left[1 - \frac{1}{8}(\Delta k_y)^2\right]^2. \tag{13.16}$$

We introduce now a new frequency

$$\Omega^2 = \omega^2 - 4, \tag{13.17}$$

and get

$$\Omega^2 - k_x^2 + \frac{1}{12}k_x^4 + (\Delta k_y)^2 = 0. \tag{13.18}$$

By using

$$\Omega^2 - k_x^2 = (\Omega - k_x)(\Omega + k_x) \simeq 2k_x(\Omega - k_x)\,,$$

we arrive finally at the dispersion relation

$$2k_x(\Omega - k_x) + \frac{1}{12}k_x^4 + (\Delta k_y)^2 = 0, \tag{13.19}$$

corresponding to the linear weakly dispersive 2d wave equation for the compression density

$$\frac{\partial}{\partial x}\left[\frac{\partial}{\partial t} + v_0\frac{\partial}{\partial x} + \frac{v_0\sigma^2}{24}\frac{\partial^3}{\partial x^3}\right]\rho(x, y, t) = \frac{v_0}{2}\frac{\partial^2}{\partial y^2}\rho(x, y, t). \tag{13.20}$$

This is nothing else than a linear version of the KP equation. By comparing our weakly dispersive 2d wave equation (13.20) with the KP equation (13.8) we see that a nonlinear term on the r.h.s is missing. By adding this term which is known to us

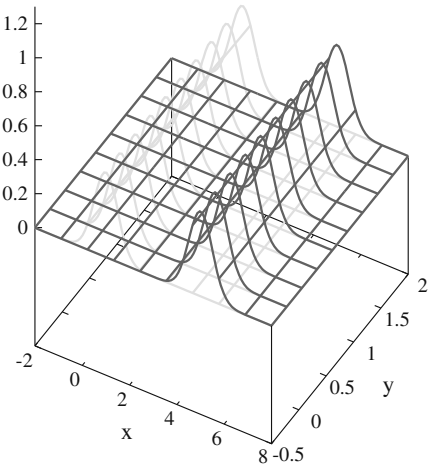


Fig. 13.4 Travelling line soliton solution of the KP equation at two successive time instants ($t = 2$, *red*, $t = 10$, *green*)

already from the Boussinesq equation we find the KP equation in physical variables as used e.g. for the description of shallow water waves [25] (Fig. 13.4):

$$\frac{\partial}{\partial x}\left[\frac{\partial}{\partial t} + v_0\frac{\partial}{\partial x} + \frac{v_0\sigma^2}{24}\frac{\partial^3}{\partial x^3}\right]\rho(x, y, t) = \frac{v_0}{2}\frac{\partial^2}{\partial y^2}\rho(x, y, t) - v_0\gamma\frac{\partial^2}{\partial x^2}\rho^2(x, y, t). \tag{13.21}$$

This equation is also exactly solvable as found by Zakharov and Shabat [55] and others [25, 33]. However the structure of the manifold of solutions is much richer than that of the BKdV equation [25]. There exist line solutions which are localized along certain lines in two-dimensional planes. These solutions are plane waves which in simplest case are generalizations of the BKdV-solitons (Fig. [33]). There exist many other line solutions [25]. A second class of solutions represent the so-called lump solitons which are like moving hills. A special solution for the envelope of a lump-type soliton reads [1, 29, 33]:

$$\rho(x, y, t) = \rho_0\frac{\left[v_s y^2 + 3/v_s - (x - v_s t)^2\right]}{\left[v_s y^2 + 3/v_s + (x - v_s t)^2\right]^2}. \tag{13.22}$$

Note that this special solution depends only on one parameter v_s which is the soliton velocity and has positive and negative parts. This is related to the property that the integral is zero

$$\int dxdy\rho(x, y, t) = 0;\ \rho_0 = \frac{v_s}{3}. \tag{13.23}$$

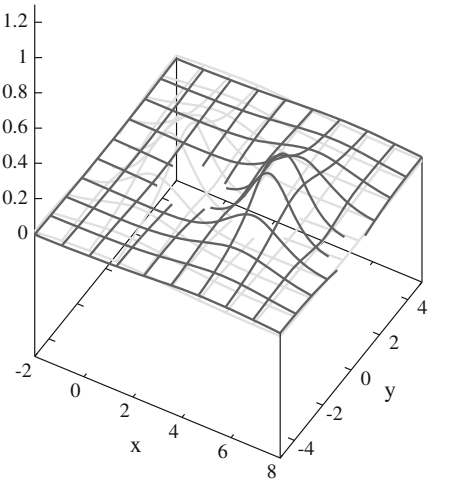


Fig. 13.5 Lump soliton solution of the KP equation at two successive time instants ($t = 0$, *red*, $t = 5$, *green*)

In Fig. 13.5 we display the envelope of a lump soliton at two subsequent time instants. Such lump solutions we have found numerically for Morse lattices in Sect. 13.2 and in [10, 11].

We come to the conclusion that the solitons found in our computer simulations for Morse lattices correspond well to the envelope of lump solitons. Recalling that we here have considered only inter-site, acoustic vibrations, it seems of interest to note that adding on-site vibrations play a stabilizing role of (longitudinal) lattice excitations (in our case solitons). In studies of high-T_c superconducting cuprates (typical 2d lattices) a bistable fourth-order on-site potential has been used for a similar purpose [4–6, 38, 39].

13.4 Tight-Binding Dynamics of Charges Interacting with the Lattice Atoms

In the triangular lattice, which is the simplest stable lattice, it is not difficult to generate solitons by appropriate initial conditions [10, 11]. We were able to generate line solitons of finite length and studied their behavior at collisions. Further by exciting atoms in one row along a crystallographic axis we could generate lump solitons running along that crystallographic axis. The Hamiltonian we used for the simulations is just the same as in Sect. 13.2 with the difference that the initial conditions correspond to an equilibrium triangular lattice now. We had initially $N = 400$ particles with periodic boundary conditions, with $b\sigma = 4$. The computer simulation illustrates the case of a line soliton, which is excited by an appropriate initial condition; it is quite about a plane wave (Fig. 13.6). In Fig. 13.7 we show an example of a lump soliton which was excited by a strong kick. Starting with a lattice at rest we attributed an initial velocity $2v_0$ to just one atom located at $x = 4$, $y = 9$ in direction of the x-axis. The

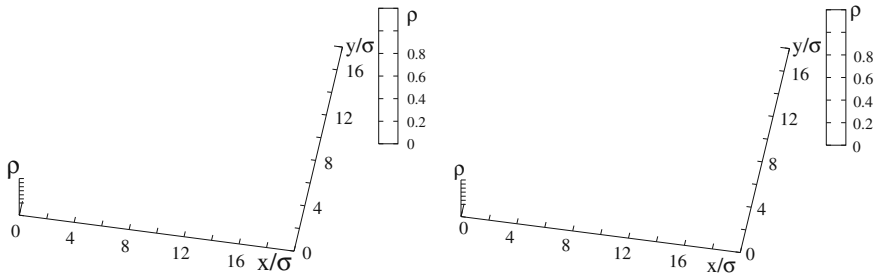
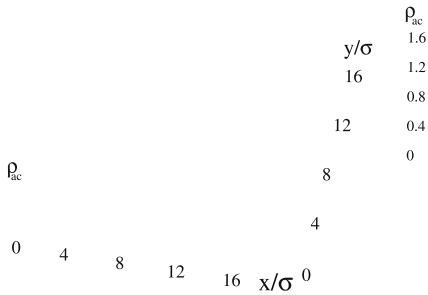


Fig. 13.6 *Triangular lattice* Line soliton excited at $t = 0$ (*left panel*) and then travelling along the x-axis. The state at $t = 5$ is at the *right panel*. Deformations of the soliton are due to the unavoidable influence of boundaries as the wave front and the direction of the velocity are not orthogonal in a triangular lattice. Focusing on the displacement of the plane wave soliton central part allows an estimate of its velocity as $1.5v_0$. *Parameter values* $N = 400$, $b\sigma = 2, \kappa = 0.465$. The excitation moves with supersonic velocity

Fig. 13.7 *Triangular lattice* Moving supersonic soliton-like compression density along a crystalographic axis. *Parameter values* $N = 400$, $b\sigma = 4$. The excitation moves with supersonic velocity



corresponding momentum is transmitted to the next neighbor at right and so on and this way a solitonic excitation is created.

Following earlier work [7, 9, 12] we will show now that lump solitons are able to carry electrons (or holes) surfing on the compression wave. We consider a system consisting of atoms arranged initially on a triangular lattice and additional electrons moving from site to site and interacting with the atoms. In order to study the evolution of the quantum states of the additional electrons interacting with the atoms in the 2d-lattice, we assume the TBA description. Let n, m denote the internal quantum numbers of the states of electrons bound to the corresponding atoms at sites $\mathbf{r}_n$ and $\mathbf{r}_m$. In the following we will assume for simplicity, that there is only one quantum state per atom which can be occupied by the added, excess electrons. If necessary, the internal state that characterizes the orbit as well as spin, can be included in the quantum number n. We set the electronic Hamiltonian as

$$H_e = \sum_n E_n c_n^+ c_n + \sum_{n,n'} t_{n,n'} c_{n'}^+ c_n. \tag{13.24}$$

The energy levels E_n will be approximated by constant values $E_n = E_0$. The transition matrix elements $t_{n,n'}$ depend in our model on the atomic distances, $t_{n,n'} = t(\mathbf{r}_{n'} - \mathbf{r}_n)$. Following Slater and others we take an exponential dependence

$$t_{n,n'} = V_0 \exp[-\alpha_h |\mathbf{r}_n - \mathbf{r}_{n'}|]. \tag{13.25}$$

The range parameter α_h can be related to the tunneling probability that decreases exponentially with distance.

For the lattice part, the Hamiltonian with Morse interactions reads as in previous sections. As before the characteristic length determining the repulsion between the particles in the lattice is σ. We limit ourselves to nearest-neighbors only using the relative distance with $r_{kj} = |\mathbf{r}_k - \mathbf{r}_j|$. Also as before by imposing the cutoff of the potential at 1.5σ, we exclude unphysical cumulative interaction effects arising from the influence of lattice units outside the first neighborhood of each atom [9, 12]. Introducing complex coordinates $Z_n = x_n + iy_n$ we write the discrete Schrödinger equation for the electrons and the Newton equations for the atoms in the form

$$\frac{dc_n}{dt} = i\tau \exp(\alpha b\sigma) \sum_{m\neq n, |Z_n - Z_m|<1.5} c_m \exp(-\alpha |Z_n - Z_m|), \tag{13.26}$$

$$\begin{aligned}\frac{d^2 Z_n}{dt^2} = &\sum_{m\neq n, |Z_n - Z_m|<1.5} [\exp(b\sigma - |Z_n - Z_m|)\,(1 - \exp(b\sigma - |Z_n - Z_m|)) \\ &+ 2\alpha V_0 \exp(\alpha(b\sigma - |Z_n - Z_m|)) Re(c_n c_m^*)] \frac{Z_n - Z_m}{|Z_n - Z_m|},\end{aligned} \tag{13.27}$$

with ($\tau = V_0/\hbar\omega_0$).

For the simulations we use again dimensionless units, i.e., lengths are measured in units σ, time in units of the reciprocal frequency around the minimum of the atomic interaction potential $1/\omega_0$. As before, for a better visualization we replace all points resulting from the simulations by little Gaussian balls representing the wave functions at the corresponding site. First we focus on the electron placed at the initial time instant at a site far from its possible disturbance of the velocity of a lattice particle, hence evolving as in a boundless unperturbed lattice (Fig. 13.8, left panel, $t = 0.2$). The system of eigen-modes of the lattice, with the soliton in a reduced simulation domain, is formed in accordance with the boundary conditions (Fig. 13.8, right panel, $t = 0.4$). It (the soliton) evolves in time with a slow motion relative to the fast dynamics of the electron wave function. Surprinsingly enough the electron density is all gathered by the soliton and both move together as further illustrated in Fig. 13.9.

The computer simulations are carried out by solving numerically the set of equations given above for 400 atoms and 1 electron. We are well aware that simulations for a matrix of 20 to 20 sites demands a careful check for finite size effects. Preliminary tests with 1600 particles (in part presented in the next section) have however

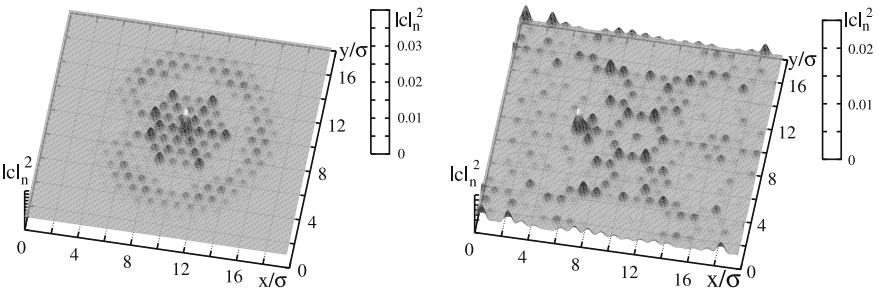


Fig. 13.8 Triangular lattice. *Left panel* Spreading of the smoothed density distribution of an electron at $t = 0.2$ which was inserted at $t = 0$ at just one lattice point. Besides the typical spreading of the wave function, we see some structuring which is due to the lattice symmetry with 3 crystallographic axes and to the periodic b.c. ($N = 400, b\sigma = 4, \tau = 10$). *Right panel* The electron feels the compression created by the running soliton and starts to concentrate around the latter ($t = 0.4$)

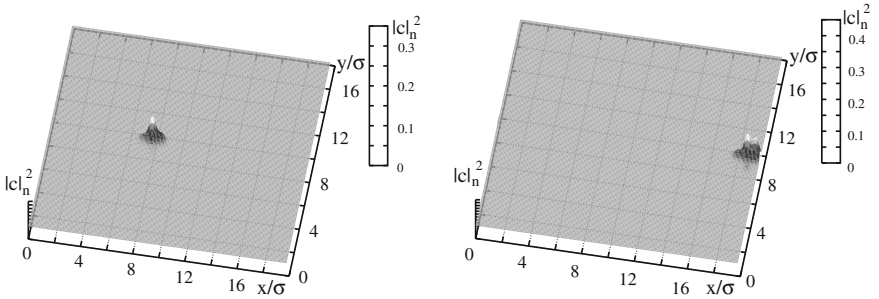


Fig. 13.9 *Triangular lattice* (follow-up of Fig. 13.8). *Left panel* Some time after, the electron is attracted by the compression created by the soliton and concentrates around the latter (*left panel*). With increasing time ($t = 5.0$) the electron density is fully concentrated around the compression density and moves with the soliton with supersonic velocity along the crystallographic axis (*right panel*)

shown that the basic effect demonstrated here, the formation of moving bound states between lattice excitations and electrons is only weakly size dependent. We note that similar phenomena of collecting electron density by solitons in nonlinear 1d- and in 2d-lattices were recently observed also by Cisneros-Ake et al. [16].

13.5 Control of Electrons and Losses-Free Transport on Longer Distances

The numerical experiments described here offer similarity with recent experiments about controlling electrons by strong surface acoustic waves [23, 32]. However a direct comparison of our simulations for small lattices with the experiments on the millimeter—scale [23, 32] is not possible. However the basic mechanism (polarization field wave) of coupling electron-lattice excitations remain the same [8, 46, 48].

Accordingly, we have a new way of charge transfer from a point A in a 2d-layer to a point B provided both points are located along a common crystallographic axis. As shown in Fig. 13.9, the soliton is able through the formation of a solectron bound state to carry an electron nearly free of losses at least on a distance of 20 crystallographic units, i.e. possibly around 10 nm in a time interval of $t \simeq 6$ in units of the oscillation time ω_0^{-1}. Over this relatively short time and short distance no damping is seen, i.e. the transfer is nearly losses-free. We see, that the 2d-solectron propagating along a crystallographic axis which is the carrier of the observed effect is a nearly conservative process. This is connected with several circumstances:

(i) In the longitudinal direction i.e. along the axis of propagation, the soliton is a 1d- ballistic excitation for which energy is conserved.

(ii) In perpendicular direction, i.e. across the crystallographic axis of propagation, the excitations are breather-like, i.e. they are in a window of non-transparency and cannot propagate. This is related to the dispersion relations discussed in Sect. 13.4.

Of course, some losses cannot be avoided, however the losses are for this kind of charge transfer very weak in comparison with standard ways of charge transfer which are connected with the emission of phonons preferentially in perpendicular direction. In our case, the phonon emission is weak due to fact that in the operating regime, phonons are in the window of non-transparency.

In order to study the actual losses and the life time of solectronic excitations in more detail, we studied a sample with a rather long channel-like two-dimensional crystal containing $N = 20 \cdot 80 = 1600$ particles. Looking at Fig. 13.10 we see

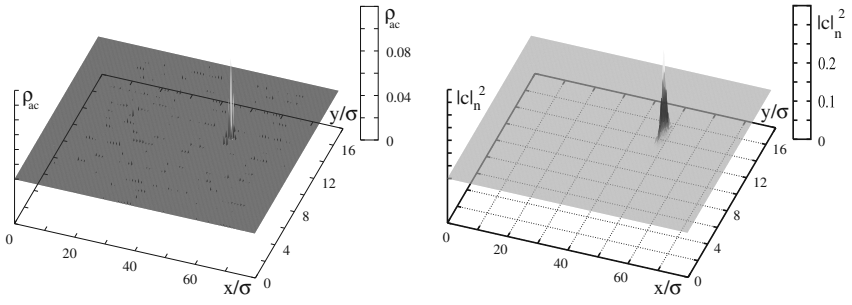


Fig. 13.10 *Triangular lattice* Soliton compression density (*left panel*) and corresponding electron probability density (*right panel*) in a channel-like lattice of $N = 20 \cdot 80 = 1600$ particles after a relatively long time of propagation $t = 50$ ($b\sigma = 4$). The soliton was created by attributing to one atom at $x = 10$, $y = 9$ in a lattice at rest the velocity $2v_0$ in $x-$ direction. The compression density (*left*) and the charge probability density (*right*) coincide very well even after a relatively long time of propagation $t = 50$

(i) the transverse extension similar as predicted by the lump solution of the KP equation (13.22),

(ii) the absence of significant losses leading to a nearly ballistic propagation. Note that the directed motion of an electron guided by a soliton along crystallographic axis may carry a current [22, 51]. In order to study the effect of an electric field we may add a corresponding term to the TBA equations as in [22, 51]. We shall deal with these problem elsewhere. The value of the electron drift velocity is determined mainly by the velocity of the carrier, the soliton.

13.6 Discussion

We have studied the dynamics of soliton-like excitations in several two-dimensional lattices: square and triangular lattice including interaction with charges. First, we have discussed dispersion laws of 2d solitons and basic solutions of the KP theory and compared them to computer simulations. Further we have developed theoretical tools for the study of *slaved* or *controlled* individual electron evolution by means of lattice soliton-like excitations. The latter act as carriers along the crystallographic axes of, e.g., a triangular lattice. The velocity of solectrons may be higher than a km/s (Å/ps) in a crystal hence, faster than the drift velocities of "free" electrons, which usually do not exceed $1 - 100$ cm/s. Such high electron velocities were observed experimentally in crystals of PDA and PDTA by Donovan and Wilson [18, 19, 47, 53]. Therefore there is experimental evidence that solitonic excitations may create bound states which are able to carry electrons at near-to-sound velocity (above and below) over a distance of a few hundred sites. This appears as a clear case of electron surfing and mathematically speaking connects similar phenomena at the macro-level in piezoelectric substrates, where a carrier polarization field wave comes as consequence of the acoustic (linear and better soliton) wave. Finally, a most interesting result is, that due to the practically conservative character of the lattice soliton motion and the low radiation of lump solitons in transverse directions, the electron transfer or transport (with eventual current) is nearly losses-free.

Acknowledgments The authors acknowledge fruitful discussions and correspondence with A.S. Alexandrov (deceased), V.S. Anishchenko, L. Brizhik, A. Bussmann-Holder, L.A. Cisneros-Ake, L. Cruzeiro, S. Dmitriev, D. Hennig, J.P. Launay, D.M. Newns, G. Röpke and F.M. Russell. The authors also wish to thank V.I. Nayanov, C. Ford, A. Wixforth, R.P.G. McNeil, and T. Meunier for sharing with us their nonlinear acoustic wave and electron surfing experiments in piezoelectric layers. E.G. Wilson and K. Donovan are also gratefully acknowledged for detailed information on their experiments on charge motion in PDA and related crystals. This research was supported by the Spanish Ministerio de Ciencia e Innovacion, under Grant MAT2011-26221 and by the Ministry of Education and Science of the Russian Federation within FTP Scientific and pedagogical personnel of the innovative Russia, 2009-2013, grant 14.B37.21.0751.

References

1. Ablowitz, M.J., Clarkson, P.A.: Solitons, Nonlinear Evolution Equations and Inverse Scattering, vol. 149. Cambridge University Press, Cambridge (1991)
2. Anishchenko, V.S., Astakhov, V., Neiman, A., Vadivasova, T., Schimansky-Geier, L.: Nonlinear Dynamics of Chaotic and Stochastic Systems: Tutorial and Modern Developments. Springer Science & Business Media, Berlin (2007)
3. Aubry, S.: Breathers in nonlinear lattices: existence, linear stability and quantization. Physica D **103**(1), 201–250 (1997)
4. Bussmann-Holder, A., Bishop, A.R.: Anharmonicity-induced multiphonon processes in high-temperature superconductors. Phys. Rev. B **44**(6), 2853 (1991)
5. Bussmann-Holder, A., Bishop, A.R.: Role of electron-two phonon interaction in ferroelectrics and oxide superconductors. Ferroelectrics **128**(1), 99–104 (1992)
6. Bussmann-Holder, A., Simon, A., Büttner, H.: Possibility of a common origin to ferroelectricity and superconductivity in oxides. Phys. Rev. B **39**(1), 207 (1989)
7. Chetverikov, A.P., Ebeling, W., Röpke, G., Velarde, M.G.: Hopping transport and stochastic dynamics of electrons in plasma layers. Contrib. Plasm. Phys. **51**(9), 814–829 (2011)
8. Chetverikov, A.P., Ebeling, W., Velarde, M.G.: Dissipative solitons and complex currents in active lattices. Int. J. Bifurcat. Chaos **16**(06), 1613–1632 (2006)
9. Chetverikov, A.P., Ebeling, W., Velarde, M.G.: Local electron distributions and diffusion in anharmonic lattices mediated by thermally excited solitons. Eur. Phys. J. B **70**(2), 217–227 (2009)
10. Chetverikov, A.P., Ebeling, W., Velarde, M.G.: Localized nonlinear, soliton-like waves in two-dimensional anharmonic lattices. Wave Motion **48**(8), 753–760 (2011)
11. Chetverikov, A.P., Ebeling, W., Velarde, M.G.: Properties of nano-scale soliton-like excitations in two-dimensional lattice layers. Physica D **240**(24), 1954–1959 (2011)
12. Chetverikov, A.P., Ebeling, W., Velarde, M.G.: Soliton-like excitations and solectrons in two-dimensional nonlinear lattices. Eur. Phys. J. B **80**(2), 137–145 (2011)
13. Christiansen, P.L., Sorensen, M.P., Scott, A.C.: Nonlinear Science at the Dawn of the 21st Century, vol. 542. Springer Science & Business Media, New York (2000)
14. Christov, C.I., Maugin, G.A., Velarde, M.G.: Well-posed Boussinesq paradigm with purely spatial higher-order derivatives. Phys. Rev. E **54**(4), 3621 (1996)
15. Christov, C.I., Velarde, M.G.: Inelastic interaction of Boussinesq solitons. Int. J. Bifurcat. Chaos **4**(05), 1095–1112 (1994)
16. Cisneros-Ake, L.A., Minzoni, A.A., Velarde, M.G.: Variational approximation to electron trapping by soliton-like localized excitations in one-dimensional anharmonic lattices. In: Localized Excitations in Nonlinear Complex Systems, pp. 225–235. Springer, Berlin (2014)
17. Davydov, A.S.: Solitons in Molecular Systems. Reidel, Dordrecht (1991)
18. Donovan, K.J., Freeman, P.D., Wilson, E.G.: Micro-engineering of a novel organic molecular electronic structure. J. Phys. C: Solid State **18**(11), L275 (1985)
19. Donovan, K.J., Wilson, E.G.: Demonstration of an ultra-high mobility organic polymer. Phil. Mag. B **44**(1), 9–29 (1981)
20. Emery, V.J., Kivelson, S.A., Tranquada, J.M.: Stripe phases in high-temperature superconductors. Proc. Nat. Acad. Sci. **96**(16), 8814–8817 (1999)
21. Flach, S., Gorbach, A.V.: Discrete breathers-advances in theory and applications. Phys. Rep. **467**(1), 1–116 (2008)
22. Hennig, D., Chetverikov, A., Velarde, M., Ebeling, W.: Electron capture and transport mediated by lattice solitons. Phys. Rev. E **76**(4), 046602 (2007)
23. Hermelin, S., Takada, S., Yamamoto, M., Tarucha, S., Wieck, A.D., Saminadayar, L., Bäuerle, C., Meunier, T.: Electrons surfing on a sound wave as a platform for quantum optics with flying electrons. Nature **477**(7365), 435–438 (2011)
24. Kadomtsev, B.B., Petviashvili, V.I.: On the stability of solitary waves in weakly dispersing media. Sov. Phys. Dokl. **15**(6), 539–541 (1970)

25. Kodama, Y.: Kp solitons in shallow water. J. Phys. A **43**(43), 434004 (2010)
26. Kohsaka, Y., Taylor, C., Fujita, K., Schmidt, A., Lupien, C., Hanaguri, T., Azuma, M., Takano, M., Eisaki, H., Takagi, H., Uchida, S., Davis, J.C.: An intrinsic bond-centered electronic glass with unidirectional domains in underdoped cuprates. Science **315**(5817), 1380–1385 (2007)
27. Kohsaka, Y., Taylor, C., Wahl, P., Schmidt, A., Lee, J., Fujita, K., Alldredge, J.W., McElroy, K., Lee, J., Eisaki, H., Uchida, S., Lee, D.H., Davis, J.C.: How cooper pairs vanish approaching the Mott insulator in $Bi_2\ Sr_2\ Ca\ Cu_2\ O_{8+\delta}$. Nature **454**(7208), 1072–1078 (2008)
28. Kudryashov, N.A.: Methods of Nonlinear Mathematical Physics. Intellekt Publishing, Dolgoprudnyi (2010) (in Russian)
29. Manakov, S.V., Zakharov, V.E., Bordag, L.A., Its, A.R., Matveev, V.B.: Two-dimensional solitons of the Kadomtsev-Petviashvili equation and their interaction. Phys. Lett. A **63**(3), 205–206 (1977)
30. Marin, J.L., Eilbeck, J.C., Russell, F.M.: Localized moving breathers in a 2D hexagonal lattice. Phys. Lett. A **248**(2), 225–229 (1998)
31. Marın, J.L., Russell, F.M., Eilbeck, J.C.: Breathers in cuprate-like lattices. Phys. Lett. A **281**(1), 21–25 (2001)
32. McNeil, R.P.G., Kataoka, M., Ford, C.J.B., Barnes, C.H.W., Anderson, D., Jones, G.A.C., Farrer, I., Ritchie, D.A.: On-demand single-electron transfer between distant quantum dots. Nature **477**(7365), 439–442 (2011)
33. Minzoni, A.A., Smyth, N.F.: Evolution of lump solutions for the KP equation. Wave Motion **24**(3), 291–305 (1996)
34. Moler, K.A.: High-temperature superconductivity: how the cuprates hid their stripes. Nature **468**(7324), 643–644 (2010)
35. Naianov, V.I.: Surface acoustic cnoidal waves and solitons in a LiNbO3-(SiO film) structure. ZhETF Pisma Redaktsiiu **44**, 245–247 (1986)
36. Nepomnyashchy, A.A., Velarde, M.G.: A three-dimensional description of solitary waves and their interaction in Marangoni-Bénard layers. Phys. Fluids **6**(1), 187–198 (1994)
37. Nepomnyashchy, A.A., Velarde, M.G., Colinet, P.: Interfacial Phenomena and Convection. CRC Press, Roca Baton (2001)
38. Newns, D.M., Tsuei, C.C.: Fluctuating Cu–O–Cu bond model of high-temperature superconductivity. Nat. Phys. **3**(3), 184–191 (2007)
39. Nistor, R.A., Martyna, G.J., Newns, D.M., Tsuei, C.C., Müser, M.H.: Ab initio theory of the pseudogap in cuprate superconductors driven by C 4 symmetry breaking. Phys. Rev. B **83**(14), 144503 (2011)
40. Remoissenet, M.: Waves Called Solitons: Concepts and Experiments. Springer Science & Business Media, Berlin (1999)
41. Reznik, D., Pintschovius, L., Ito, M., Iikubo, S., Sato, M., Goka, H., Fujita, M., Yamada, K., Gu, G.D., Tranquada, J.M.: Electron-phonon coupling reflecting dynamic charge inhomogeneity in copper oxide superconductors. Nature **440**(7088), 1170–1173 (2006)
42. Rocke, C., Zimmermann, S., Wixforth, A., Kotthaus, J.P., Böhm, G., Weimann, G.: Acoustically driven storage of light in a quantum well (1997). arXiv:cond-mat/9704029
43. Russell, F.M., Eilbeck, J.C.: Evidence for moving breathers in a layered crystal insulator at 300 K. Europhys. Lett. **78**(1), 10004 (2007)
44. Toda, M.: Theory of Nonlinear Lattices, 2nd edn. Springer-Verlag, Berlin (1989)
45. Tranquada, J.M., Sternlieb, B.J., Axe, J.D., Nakamura, Y., Uchida, S.: Evidence for stripe correlations of spins and holes in copper oxide superconductors. Nature **375**, 561 (1995)
46. Velarde, M.G.: From polaron to solectron: the addition of nonlinear elasticity to quantum mechanics and its possible effect upon electric transport. J. Comput. Appl. Math. **233**(6), 1432–1445 (2010)
47. Velarde, M.G., Chetverikov, A.P., Ebeling, W., Wilson, E.G., Donovan, K.J.: On the electron transport in polydiacetylene crystals and derivatives. Europhys. Lett. **106**(2), 27004 (2014)
48. Velarde, M.G., Ebeling, W., Chetverikov, A.P.: On the possibility of electric conduction mediated by dissipative solitons. Int. J. Bifurcat. Chaos **15**(01), 245–251 (2005)

49. Velarde, M.G., Ebeling, W., Chetverikov, A.P.: Soliton-mediated compression density waves and charge density in 2d layers of underdoped cuprate-like lattices. C. R. Mecanique **340**(11), 910–916 (2012)
50. Velarde, M.G., Ebeling, W., Chetverikov, A.P.: Localized excitations and anisotropic directional ordering in a two-dimensional Morse lattice model of cuprate layers. In: Localized Excitations in Nonlinear Complex Systems, pp. 213–224. Springer, Berlin (2014)
51. Velarde, M.G., Ebeling, W., Chetverikov, A.P., Hennig, D.: Electron trapping by solitons: classical versus quantum mechanical approach. Int. J. Bifurcat. Chaos **18**(02), 521–526 (2008)
52. Volk, S., Schulein, F.J., Knall, F., Reuter, D., Wieck, A.D., Truong, T.A., Kim, H., Petroff, P.M., Wixforth, A., Krenner, H.J.: Enhanced sequential carrier capture into individual quantum dots and quantum posts controlled by surface acoustic waves. Nano Lett. **10**(9), 3399–3407 (2010)
53. Wilson, E.G.: A new theory of acoustic solitary-wave polaron motion. J. Phys. C: Solid State **16**(35), 6739 (1983)
54. Zaanen, J.: Superconductivity: quantum stripe search. Nature **440**(7088), 1118–1119 (2006)
55. Zakharov, V.E., Shabat, A.B.: A scheme for integrating the nonlinear equations of mathematical physics by the method of the inverse scattering problem. I. Funct. Anal. Appl. **8**(3), 226–235 (1974)
56. Zolotaryuk, A.V., Spatschek, K.H., Savin, A.V.: Supersonic mechanisms for charge and energy transfers in anharmonic molecular chains. Phys. Rev. B **54**(1), 266 (1996)